Longitudinal Coupling Impedance of a Thin Iris Collimator*

R.L. Gluckstern and W.F. Detlefs
Department of Physics, University of Maryland, College Park, MD 20742

I. INTRODUCTION

We present here the results of numerical calculations of the longitudinal coupling impedance of a thin iris collimator in a beam pipe. The calculations are performed using an analytic result derived in a previous note[1]. The impedance is calculated as a function of frequency ($kc/2\pi$) and inner and outer radius ($r = b$ and $r = a$). The results are presented by plotting the admittance as a function of $k(a-b) = kax$ for different $x \equiv (a-b)/a$. Comparison is made with the expected behavior of the admittance in the small iris limit ($x \ll 1$).

II. ANALYTIC RESULT

We now summarize the derivation of the analytic result given in the previous research note[1]. We began by writing the electromagnetic fields as the sum of a source term plus transmitted and reflected modes in the beam pipe. The fields were then matched at $z = 0$ (the axial location of the iris) to obtain an integral equation for the discontinuity in the axial electric field from one side of the iris to the other. Finally the following variational form was constructed for the admittance

$$Z_oY(k) = \frac{\int_b^a rdr \int_b^a r'dr' \, g(r)\, g(r')\, K(r,r)}{\left[\int_b^a rdr \, g(r)\, \ell n(a/r)\right]^2}, \qquad (1)$$

where $g(r)$ is a trial function proportional to the discontinuity in the axial electric field, and $K(r,r')$ is the kernel of the integral equation, given by

$$K(r,r') = \frac{2\pi}{k}\sum_{i=1}^{\infty}\frac{\beta_i J_o(p_i r/a)\, J_o(p_i r'/a)}{J_1^2(p_i)}. \qquad (2)$$

Here p_i are the zeros of $J_o(u)$ and

$$\beta_i a = (k^2a^2 - p_i^2)^{1/2} = -j(p_i^2 - k^2a^2)^{1/2}. \qquad (3)$$

The solution to the integral equation was obtained by expanding the discontinuity in magnetic field in terms of the complete set $F_1(\sigma_m r)$ in the interval $b \le r \le a$, where

$$F_1(\sigma_m r) = Y_1(\sigma_m r) - \frac{Y_o(\sigma_m a)}{J_o(\sigma_m a)} J_1(\sigma_m r) \qquad (4)$$

and where the eigenvalues σ_m satisfy $F_1(\sigma_m b) = 0$. The final result for the impedance was

$$\frac{Z(k)}{Z_o} = \sum_m \sum_m (P^{-1})_{mn}, \qquad (5)$$

where $Z_o = 120\pi$ ohms is the impedance of free space and the m,n element of the symmetric matrix P is given by

$$P_{mn} = \frac{2\pi b^2}{ka^2}\sum_i \frac{J_1^2(p_i \frac{b}{a})}{J_1^2(p_i)} \frac{\sigma_m^2 a^2}{\sigma_m^2 a^2 - p_i^2}\cdot\frac{\sigma_n^2 a^2}{\sigma_n^2 a^2 - p_i^2}. \qquad (6)$$

Truncation of the series in Eq. (6) is not expected to significantly affect numerical accuracy, since the result was obtained using the variational form in Eq. (1).

III. SMALL IRIS LIMIT

It is easy to show from the variational form for $Z_oY(k)$ that[1]

$$Z_oY(k) = Z_oG(k) + jZ_oB(k) \cong \frac{\pi}{2}ka - \frac{j\,Aa}{k(a-b)^2} \qquad (7)$$

is the limiting form for the admittance for a small iris ($x \ll 1$, or $a-b \ll a$). Here A is expected to be weakly dependent on ka and of order 1.

The small x approximation in Eq. (7) has two interesting features. The first is that $G(k)$, the real part of the admittance, is independent of the geometry of the obstacle. The second is that $B(k)$, the imaginary part of the admittance, is inversely proportional to the cross-sectional area in the $r-z$ plane where the field is significantly disturbed by the iris (approximate dimensions $a-b$ by $a-b$). These features are the same as those encountered in the case of a small convex obstacle in a beam pipe[2], where the corresponding result was

$$Z_o\tilde{Y}(k) \cong \pi\, ka - \frac{2\pi\, ja}{k\Delta}, \qquad (8)$$

*Work supported by the Department of Energy.

0-7803-0135-8/91$03.00 ©IEEE

where Δ is the cross-sectional area of the obstacle. We speculate that these features are part of a more general result which will also apply for a small iris of small but finite thickness and possibly even general shape.

Finally we can also examine the high frequency limit for a small iris where kax may be of order 1 or greater. The form of the result can most easily be seen by taking the corresponding limit in Eq. (6) where $J_1(p_i b/a)/J_1(p_i)$ goes over to $cos p_i x$, the equivalent 2-D result. The prediction is then that $xZ_oY(k)$ will be a function of the universal variable kax. The small kax limit is that given in Eq. (7), namely

$$xZ_oY(k) \cong \frac{\pi}{2}\ kax - \frac{j\ A}{kax}\ ,\ kax \ll 1 \tag{9}$$

and the large kax limit can be obtained via Eq. (6), and is

$$xZ_oY(k) \simeq \pi - \frac{2j}{kax}\ ,\ kax \gg 1. \tag{10}$$

IV. CONVERGENCE BEHAVIOR

The convergence of the analytic method was examined with respect to truncation of the series in Eq. (6) and with respect to the size of the matrix P. To check the convergence of the series, we set $b = 0.9, a = 1.0$ and chose values for ka and n, where $n \times n$ is the matrix size. (Note: throughout the rest of this paper the length scale is chosen so that $a = 1.0$). The values of ka used here were between 10 and 100, and $n = 20, 25$, or 30. We then calculated the admittance for different values of i_{max}, the maximum value of the index in Eq. (6). The real and imaginary parts of the admittance were then plotted as a function of $1/i_{max}$. This procedure was repeated for different values of ka and n. The resulting plots indicated that the convergence was linear in $1/i_{max}$, which was the expected behavior. This allowed for a simple linear extrapolation to estimate the error in the admittance due to the truncation of the series. We determined that a value of $i_{max} = 5000$ would give an error due to truncation of approximately one part in 10^5, which is negligible in comparison with the error due to finite matrix size (discussed below). All calculations referred to throughout the rest of this paper were performed using $i_{max} = 5000$.

To determine the dependence of the calculated admittance on matrix size, we let $b = 0.9$ and chose a value for ka. We then calculated the admittance for $n = 10, 15, 20, 25$, and 30. The real and imaginary parts of the admittance were then plotted as a function of $1/n$. This procedure was repeated for different values of ka. The resulting plots revealed a strong linear dependence on $1/n$ as well as a dependence on higher-order terms in $1/n$. We determined that a quadratic interpolation would give the best results for the admittance, resulting in an error of no more than one part in 10^2.

V. NUMERICAL RESULTS

The numerical results are presented in Figures 1-4. Equation (9) suggests that $xZ_oY(k)$ is primarily a function of kax for $kax \ll 1$. We therefore plot $xZ_oG(k)$ (Figure 1) and $kax^2Z_oB(k)$ (Figure 2) versus kax for $x = .05, .1, .3$. The plots do show the behavior expected from Eqs. (9) and (10). In Fig. 1, we plot the line with slope $\pi/2$ and the horizontal line with ordinate π; it is then easily seen that the calculated values for $G(k)$ are consistent with Eqs. (9) and (10). The fact that the curves in Figs. 1 and 2

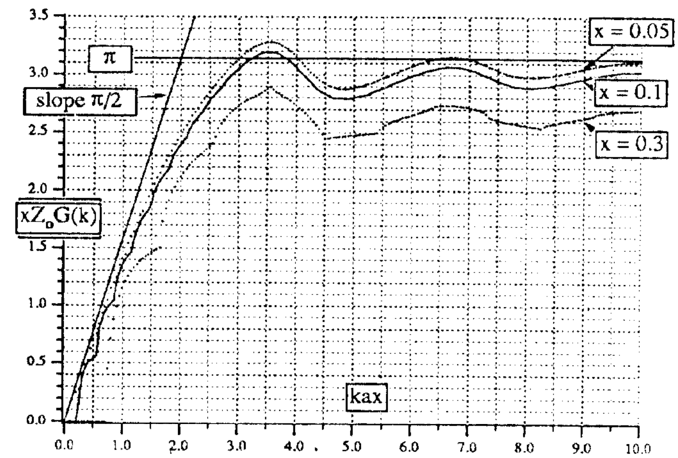

Figure 1: Real part of the admittance (multiplied by x) vs. kax for small x.

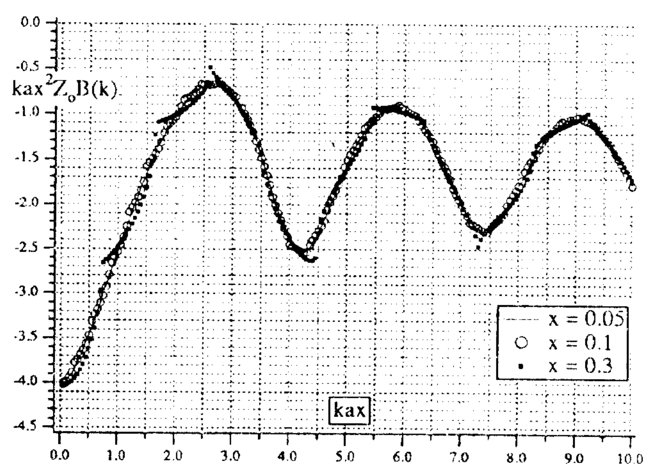

Figure 2: Imaginary part of the admittance (multiplied by kax^2) vs. kax for small x.

lie very close to each other suggests that for small x, the calculated values for the impedance are universal, that is, a function only of kax (except for an overall factor x). It should be noted that Fig. 2 suggests the value of A in Eq. (9) is close to 4.

Figs. 3 and 4 explore the departure from Eq. (9) as x becomes of order 1. In Fig. 3 we plot $xZ_oG(k)$ versus

kax for x = .05, .5, .7, and .9. The curves show roughly the same oscillatory behavior as in Fig. 1, in the sense that the minima and maxima occur at the same locations. As expected, as x increases the curves depart significantly from the result for small x.

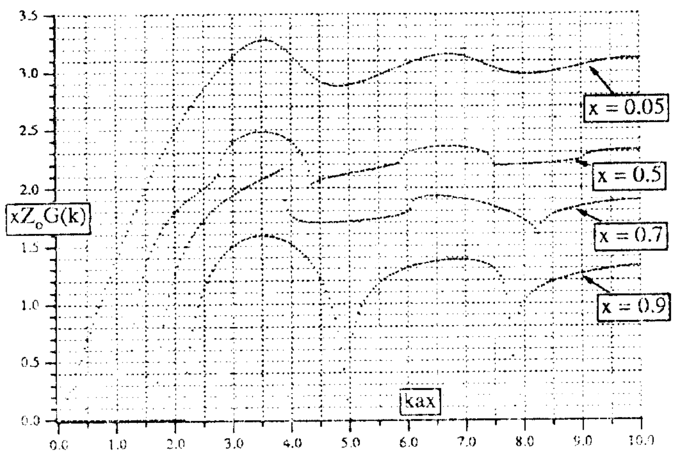

Figure 3: Real part of the admittance (multiplied by x) vs. kax for large x.

In Fig. 4 we plot $xZ_oB(k)$ versus kax for x = .05, .5, .7, and .9. We see roughly the same oscillatory behavior as in Fig. 2. It should be noted from Eq. (10) that for x close to 1 and large kax, $B(k)$ will be small compared to $G(k)$ and the impedance will be approximately real. The calculated values are consistent with this conclusion.

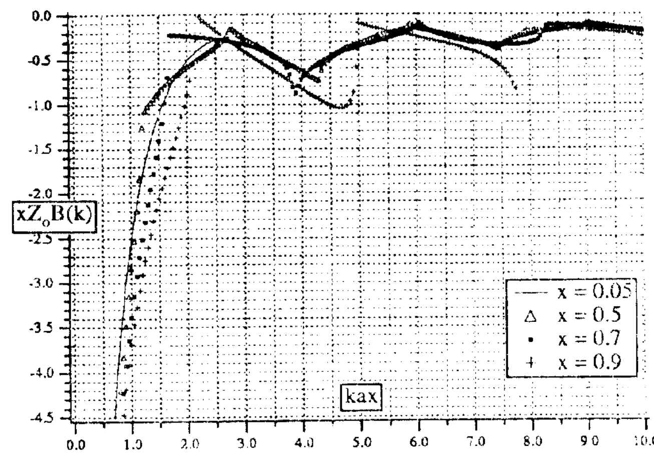

Figure 4: Imaginary part of the admittance (multiplied by x) vs. kax for large x.

VI. ACKNOWLEDGMENT

One of the authors (WFD) is grateful to Johannes van Zeijts for helpful discussions.

VII. REFERENCES

[1] R.L. Gluckstern, Longitudinal Coupling Impedance of an Iris in a Beam Pipe, CERN research note CERN SL/90-113 (AP).

[2] R.L. Gluckstern and F. Neri, Longitudinal Coupling Impedance of a Small Obstacle, Proceedings of the Particle Accelerator Conference, Chicago, IL, p. 1271 (1989).